Inter-Research Science Publisher

Marine Ecology Progress Series
Volume 785:meps15153

Published May 13, 2026
https://doi.org/10.3354/meps15153

FEATURE ARTICLE

Seasonal residency and large-scale return migration patterns of basking sharks in high-latitude environments of the North Atlantic

C. Antonia Klöcker[1,2,✉], Martin C. Arostegui[3], Keno Ferter[1], Otte Bjelland[1], Mauvis A. Gore[4,5], Jan Hiriksson[1], Robert J. Lennox[6], Petter Lundberg[7], Peter I. Miller[8], Axel Schlindwein[9], Lara L. Sousa[10,11,12], David W. Sims[13,14], Nuno Queiroz[10,11,#], Claudia Junge[1,#,✉]

[1]Havforskningsinstituttet (Institute of Marine Research, IMR), 5005 Bergen, Norway
Full author addresses are given in the Appendix

ABSTRACT: Marine megafauna adopt diverse movement strategies to balance the costs and benefits of migration amid shifting environments, resources, and reproductive demands. Species with broad latitudinal ranges can exhibit distinct movement patterns at the edges of their distribution. However, pan-latitudinal perspectives on annual movements remain scarce, as exemplified by the planktivorous basking shark *Cetorhinus maximus*, for which most data derive from temperate waters near the range centre. We satellite-tracked 13 basking sharks tagged near their northern distributional limit in northern Norway for up to 515 d to investigate year-round horizontal and vertical movements. Six of 7 sharks, each tracked for ≥338 d, performed large-scale return movements — departing the Norwegian shelf after summer, occupying the West European Basin and adjacent waters during winter, and returning to the Norwegian Sea the following summer. Individuals covered annual distances averaging ~14 000 km, including one transatlantic movement to the southern Sargasso Sea. Vertically, sharks exhibited irregular surface use and isobath tracking in boreal shelf habitats, and mesopelagic occupancy with diel vertical migration in lower-latitude oceanic waters, consistent with known prey distributions. Seasonal movements averaged 30° of latitude, exceeding those of lower-latitude conspecifics, thereby providing first evidence of 'leapfrog migration' in basking sharks. These comparably consistent latitudinal movements likely track large seasonal shifts in prey availability within a 2–25°C thermal envelope. As climate change and other anthropogenic pressures alter marine habitats and phenologies, these findings advance understanding of range-edge movement dynamics and underscore the value of long-term, pan-latitudinal studies for assessing population connectivity and guiding dynamic conservation strategies for this endangered megaplanktivore.

KEY WORDS: *Cetorhinus maximus* · Lamniformes · Inter-annual site fidelity · Hotspot · Philopatry · Diel vertical migration · DVM · Thermal niche · Biotelemetry · Geolocation

Drone image of a basking shark (*Cetorhinus maximus*) filter-feeding in surface waters around the Lofoten peninsula in northern Norway.

Photo: C. Antonia Klöcker, Havforskningsinstituttet

✉ Corresponding authors: kloecker.c.a@gmail.com, claudia.junge@hi.no
#These authors contributed equally to this work

Publisher: Inter-Research · www.int-res.com

1. INTRODUCTION

Marine megafauna such as planktivorous sharks and whales exhibit diverse, habitat-dependent movement strategies (Sequeira et al. 2018). Despite most megafauna being highly mobile and capable of far-ranging movements, patterns of residency, site fidelity, and philopatry are surprisingly common and known to structure populations (Hueter et al. 2005, Chapman et al. 2015). Behavioural strategies such as residency or migration can be expected to result from cost–benefit trade-offs (Dingle 2014). At the individual level, migratory lifestyles are favoured if the costs of migration — e.g. due to transport (Wikelski et al. 2003), elevated predation pressure (Béguer-Pon et al. 2012), or reduced feeding opportunities (Chapman et al. 2013) — are outweighed by benefits of moving to alternative habitat such as greater resource provisioning or reproductive success. In addition to habitat heterogeneity, fitness benefits are modulated by intrinsic (e.g. ontogeny, sex, reproductive state, genetic disposition) and extrinsic biotic factors (e.g. competition, predation risk, parasite load), resulting in intraspecific variability of horizontal movement strategies (Alò et al. 2021). Such variation can manifest as differences in migration propensity, as in partial migration, where only some individuals within a population migrate while others remain resident (Chapman et al. 2012, Papastamatiou et al. 2013, McMillan et al. 2019), or as differences in the timing or destination of migration among demographic groups (differential migration). As seasonal fluctuations in resource availability intensify with latitude, migration extent can also differ among populations occupying different latitudes (e.g. during the breeding season), giving rise to chain, telescopic, or leapfrog patterns (Chapman et al. 2014).

The basking shark *Cetorhinus maximus* presents a compelling case study for investigating context-dependent movement strategies. This highly mobile, pelagic megaplanktivore is circumglobally distributed, with its distribution centred in temperate waters (Sims 2008). Tracking studies have documented large-scale movements in this species, including transatlantic and transequatorial movements (Gore et al. 2008, Skomal et al. 2009, Braun et al. 2018b, Johnston et al. 2019), and, together with genetic studies, suggest patterns of seasonal residency and interannual site fidelity (Sims et al. 2003, 2006, Gore et al. 2016, Doherty et al. 2017b, Dolton et al. 2020, Lieber et al. 2020, Thorburn et al. 2024).

Most knowledge of *C. maximus* movement dynamics comes from individuals inhabiting temperate waters, particularly around the British Isles, where extensive tagging efforts have shown sharks to forage in productive shelf areas during summer (Sims & Quayle 1998, Sims et al. 2005, 2006, Miller et al. 2015, Doherty et al. 2017b). Although fewer data exist for the post-summer period, available evidence indicates considerable variability in horizontal movement patterns during this period, with some individuals remaining in British or Irish waters and others exhibiting southward movements of up to ~20° in latitude to oceanic habitats along the Iberian and Moroccan coasts (Sims et al. 2003, Doherty et al. 2017a, Dolton et al. 2020, Johnston et al. 2022).

Beyond this comparably well-studied *C. maximus* 'hotspot' in the Northeast Atlantic (NEA), off-shelf and/or large-scale latitudinal post-summer movements have been reported in the Northeast Pacific (NEP; Dewar et al. 2018) and Northwest Atlantic (NWA; Braun et al. 2018b). However, the species' distribution extends into boreal waters, including areas around Newfoundland (Canada) and northern Norway (Lien et al. 1986, Mecklenburg et al. 2018), where annual movement dynamics remain largely unexplored.

In this study, we investigated the horizontal and vertical movement patterns of *C. maximus* tagged near their northernmost range limit (hereafter, high-latitude individuals) throughout the annual cycle. Using satellite telemetry, we aimed to (1) characterise horizontal movements of high-latitude individuals across seasons; (2) identify annual high-use areas across these individuals and determine depth and temperature use within these areas; and (3) discuss observed latitudinal movements in the context of seasonal fluctuations in temperature and secondary productivity, as well as previously reported movement patterns of *C. maximus* tagged at lower latitudes near the species' core distribution in the NEA (hereafter, lower-latitude individuals). In doing so, we expand upon existing knowledge from lower latitudes, providing new insights into the annual movement behaviour and habitat use of *C. maximus* in the NEA and wider North Atlantic.

2. MATERIALS AND METHODS

2.1. Tagging and data retrieval

Cetorhinus maximus individuals were tagged with pop-up satellite archival transmitting (PSAT) tags (miniPAT-348, Wildlife Computers) and/or Smart Position and Temperature (SPOT) transmitting tags (SPOT6-253G, Wildlife Computers) around Lofoten

and Vesterålen, northern Norway, in June and July 2022 and 2023. Each tag was fitted with a Wildlife Computers large titanium anchor (64 × 16 × 1 mm) fixed to a custom-made tether consisting of 220 lb fluorocarbon monofilament line (1.66 mm, Seaguar, Blue Label) covered with heat-shrunk plastic tubing. In the case of PSAT tags, tethers measured 15 cm to ensure a close attachment to the body with a fixed point at its cone (Klöcker et al. 2025a). For the SPOT tags, the tether was 1.5 ± 0.3 m length with ad hoc adjustment based on the shark's estimated total body length (L_T) to position the tag at the level of the second dorsal fin. To ensure the detachment of the tether and thus avoid potential entanglement risk in the long-term, the SPOT tether comprised a programmable release mechanism (PRD-TI, Wildlife Computers) close to the body, set to release after 2 yr.

Sharks were approached and tagged from behind deploying 1 tag at a time from the bow of a 10 m aluminium boat (Arronet 30 Surprise, Arronet Teknik). Where possible, the shark's L_T was assessed from drone images; otherwise, L_T was estimated visually with respect to the boat length. In addition to aerial images, underwater footage for photo and sex identification were collected. Sex was determined by the absence (female) or presence (male) of claspers. Where no underwater footage was available, sex was inferred from aerial footage via the absence (male) or presence (female) of bitemarks on pectoral fins (Fig. S1 in the Supplement at www.int-res.com/articles/suppl/meps15153_supp.pdf), typically interpreted as mating-associated scars. A 3 m tagging pole was used to insert the anchor including ~15 cm of the tether just below the posterior base of the first dorsal fin.

PSAT tags were programmed to release after 233, 235, and 365 d and to detach early if a constant depth (±2.5 m) was recorded for 5 consecutive days or if depths exceeded 1700 m. Tags were set to transmit summaries of time spent in distinct depth and temperature intervals (bins) over a 24 h period (hereafter, histogram data). The range of depth or temperature bins was chosen as follows: depth bins started at 0, 10, 20, 30, 50, 100, 150, 300, 500, 700, and 1000 m. Temperature bins started at 2, 4, 6, 8, 10, 12, 14, 16, 18, 20, 22°C. In addition, the minimum and maximum depth recorded per day was transmitted (hereafter, minmax data). Further, the tags transmitted partial time series (hereafter, series data) of depth (programmed to be transmitted without schedule) and temperature (initially 30 d on, 5 d on, 5 d off schedule) every 10 min.

Recovered tags were retrieved at sea using an Argos goniometer (CLS RXG-234, CLS). Tag recovery provided access to all summary data (e.g. histogram data) without transmission-related gaps, along with an archive file comprising all raw data recorded, including continuous time series of depth and temperature at 5 s intervals. Archival time series were aggregated into 10 min intervals to match the resolution of the series data from non-recovered tags. Data processing, analyses, and visualization were performed in R (version 4.3.2, R Core Team 2023).

2.2. Geolocation and horizontal movement

Geolocation of the PSAT data was performed using the R package 'HMMoce' (Braun et al. 2018a). This gridded hidden Markov model framework compares diverse tag-based observations with remotely sensed and data-assimilating oceanographic model products to generate likelihoods of a tagged shark's location and behaviour at each time step of its deployment. At 24 h intervals, 5 separate likelihoods were calculated. These included (1) bathymetric likelihoods derived by excluding areas shallower than the tag-recorded maximum depth in the SRTM30_PLUS global bathymetry and elevation data set (Becker et al. 2009); (2) latitude and (3) longitude likelihoods estimated from light-level data via a threshold-based algorithm (Hill & Braun 2001) implemented in the GPE2 software; (4) sea surface temperature (SST) likelihoods obtained by matching tag-measured SST values (<10 m depth) to the NOAA 0.25° Daily Optimum Interpolation SST (OISST) climate data record (Reynolds et al. 2007, Banzon et al. 2016); and (5) ocean heat content likelihoods (Luo et al. 2015) produced by comparing integrated tag-derived depth—temperature profiles with outputs from the 1/12° Global Ocean Physics Reanalysis (GLORYS; Lellouche et al. 2018). All resulting likelihood grids were resampled to a spatial resolution of 0.25°. The light-based latitude and longitude likelihoods were manually inspected and filtered to remove spurious location estimates. A subset of the deployed PSAT tags were programmed to generate and transmit daily profiles of depth and temperature, but for the remainder we leveraged the transmitted depth-temperature time series to generate comparable daily profiles. Furthermore, geolocation of sharks fitted with both PSAT and SPOT tags incorporated any high-resolution location data provided by the Argos satellite transmitter as anchor points through which the model must converge and that, therefore, reduce uncertainty on the corresponding and surrounding days (Arostegui et al. 2024). In this case, deployment days with known locations consisted of likelihood surfaces restricted to a single grid cell with a likelihood of

one (Nyegaard et al. 2023), as the error radius of numbered Argos location classes (<1500 m; Douglas et al. 2012) is markedly less than the 0.25° × 0.25° grid cell resolution used in the model.

The resulting observation likelihoods were convolved with a diffusive movement kernel for a single behavioural state. Parameter estimation of behaviour state movement used bound-constrained optimization (Byrd et al. 1995). Parameter bounds and the initial value for the movement kernel were informed by the daily displacement rates (km d^{-1}) estimated from previous telemetry studies of *C. maximus* (e.g. Braun et al. 2018b) and *Rhincodon typus* (e.g. Rohner et al. 2018). Daily posterior likelihood surfaces were then summed for each tagged individual to generate time-integrated, spatial utilization distributions (UDs) across the entire deployment period, as well as for each month. The most probable track for each deployment was calculated using the Viterbi algorithm, a global decoding solution that refines daily location estimates derived from the posterior probability surfaces (Nielsen et al. 2023).

To estimate the distance covered by each shark over the deployment as well as the daily distance to the tagging location, geographical distances were calculated between each geolocated position or the tagging site using the 'geosphere' package (Hijmans 2024). Daily distances were summed across the entire track to obtain the cumulative distance travelled by each shark.

Due to the lack of days with consecutive positions from the SPOT tags, tracks for single-SPOT tagged individuals could not be generated. The best daily numbered Argos location classes were considered for mapping.

Bathymetry features were visualized using the GEBCO 2023 Bathymetry Grid, which provides elevation data at a spatial resolution of 15 arc-seconds (GEBCO Compilation Group 2023). Maps were generated using an equidistant conic projection centred on the midpoint of the reconstructed track, preserving distances along meridians. Times of day were determined based on the most probable daily position using the R package 'suncalc' (Thieurmel & Elmarhraoui 2022).

2.3. Identification of high-use areas

To identify high-use areas across PSAT-tracked individuals, we averaged daily UDs for a given day of the year (DOY) across sharks. After rescaling the resulting UDs to a 0–1 range to ensure equal weighting of each DOY independent of sample size, UDs were summed across the full year, seasons, or months and subsequently rescaled to range from 0 to 1. To delineate annual high-use areas, the 50% UD contour of the annual raster layer was used, similar to standard procedures to estimate home ranges (Powell & Mitchell 2012). Seasons were defined as follows: June–August (summer), September–November (autumn), December–February (winter), March–May (spring). The percentage of each high-use area intersecting with the monthly or seasonal 50% UD was calculated as $P = (A(H \cap S)/A(H)) \times 100$, where $A(H \cap S)$ is the area of intersection between the high-use area (H) and the monthly/seasonal polygon (S), and $A(H)$ is the total area of the high-use area.

To estimate residency time for each shark within high-use areas and compare depth and temperature use, PSAT data were assigned to annual high-use areas based on the intersection of the annual 50% UD polygon with the most probable daily shark position.

2.4. Depth–temperature patterns and vertical movements

Depth–temperature envelopes were constructed based on available series data from both recovered and non-recovered PSAT tags using kernel density estimation via the 'MASS' package (Ripley & Venables 2023). Depth-use densities were also calculated for each high-use area for both day and night separately.

To provide thermal context and highlight differences between utilized and available temperatures within high-use areas, temperature profiles were generated both from tag-based measurements and model-based data. Tag-based temperature profiles were calculated from the series data for each metre with $n > 50$ data points per high-use area (across individuals) and smoothed with a running mean ($k = 5$). The model-based temperature profiles were calculated from monthly seawater temperatures extracted from GLORYS (Lellouche et al. 2018, CMEMS 2024b). For each modelled depth, the mean (μ) and standard deviation (σ) of temperature were calculated across each high-use area for months in which the respective area was predominantly used during the study period (H1: May–July, n = 8 sharks; H2: September–November, n = 6 sharks; H3: January–March, n = 6 sharks). In the case of H1, GLORYS profiles were restricted to shelf areas (<1000 m).

Patterns of diel vertical migration (DVM) throughout each deployment were assessed from statistical differences between daytime and night-time depths

using series data, as complete time series were not available for all sharks, precluding tests of DVM sensu stricto (Klöcker et al. 2025a). To ensure that depths were not influenced by crepuscular movement patterns and varying day lengths, daytime depths were considered between 10:00 and 14:00 h local time and night-time depths between 22:00 and 02:00 h local time following Andrzejaczek et al. (2022). Given tracking at high latitude, DVM patterns were only assessed for days with more than 2 h ($n \geq 12$ series datapoints) of day and night records. A non-parametric Wilcoxon rank-sum (Mann-Whitney *U*) test was performed for each day and shark with a significance level (α) of 0.05 to assess the presence and type of DVM. Days were classified as follows: normal DVM (nDVM) when individuals occupied significantly greater depths during daylight hours than at night; reverse DVM (rDVM) when depths were significantly greater at night compared to daytime; and no DVM when no statistically significant difference was detected between daytime and night-time depths.

2.5. Contextualizing latitudinal movement patterns

To contextualize latitudinal ranges of high-latitude individuals with those of lower-latitude individuals, we compared minimum monthly latitudes from PSAT and SPOT data in our study with those provided by Doherty et al. (2017a), who present the most comprehensive long-term data set currently available on post-summer basking shark movements in the NEA. To this end, we extracted minimum monthly latitudes for each of the 28 sharks in Doherty et al. (2017a, their Fig. 4) using WebPlotDigitizer (Rohatgi 2025) and estimated the average tagging latitude from tagging locations provided in their Table S2.

To explore latitudinal shark movements in the context of environmental fluctuations of essential ocean variables across the annual cycle and utilized habitat, monthly climatologies were calculated for SST and zooplankton biomass. Monthly SST fields were obtained from the eddy-resolving 1/12° GLORYS model (Lellouche et al. 2018, CMEMS 2024b). Distributions of potential prey biomass were obtained from the low and mid-trophic levels (LMTL) reanalysis based on the dynamic population model 1/12° SEAPODYM (Lehodey et al. 2010, 2015, CMEMS 2024a). The SEAPODYM-LMTL model simulates spatio-temporal dynamics of production and biomass of zooplankton in carbon between the surface and 1000 m depth. Monthly climatologies were generated by averaging by month over the study period at 1/4°.

The average ($\mu \pm \sigma$) monthly latitude based on PSAT and SPOT data ($n = 12$) was superimposed on the monthly climatologies aggregated across latitudes using the median within the annual 95% UD contour of all PSAT tracks. Oceanographic covariates were not extracted for estimated shark locations due to the spatial uncertainties of daily geolocated positions, which precluded fine-scale modelling of habitat preferences (Arostegui et al. 2024).

3. RESULTS

In this study, 13 basking sharks *Cetorhinus maximus* were tagged along the coast of northern Norway (66.6–68.7° N) during boreal summer in June and July 2022 and 2023, including at least 5 females and 5 males (Table 1; Fig. S1). L_T ranged from 3.5 to 8.4 m ($\mu \pm \sigma$: 6.9 ± 1.4 m). Eleven sharks were equipped with PSAT tags, of which 3 were double tagged with SPOT tags (B05, B06, B08). Two sharks were single tagged with SPOT tags (B04, B07). Four of the 11 PSAT tags were recovered, enabling the retrieval and analysis of the full archival high-resolution record stored on the tag. One PSAT did not report (B03), another only sent positions following pop-up, but did not transmit any summary data (B13). Three tags released pre-maturely (B05, B08, B11; Table 1, Fig. 1).

Geolocation estimates for double-tagged sharks were informed by available high-quality Argos positions from the SPOT tags. This, together with varying quantities of transmitted data, resulted in precision differences of geolocations. An ocean heat content likelihood was available for 100% of deployment days for recovered tags and for <75% in those not recovered, while an SST likelihood was typically available for <65% of deployment days. In contrast, light-based latitude and longitude likelihoods were available for <25% of deployment days for all but 1 deployment, resulting in larger posterior uncertainties in the longitudinal component (Table S1, Fig. S2).

3.1. Horizontal movement patterns

PSAT deployments ranged from 233 to 366 d, with an average duration of 314 ± 58 days ($\mu \pm \sigma$), resulting in 2834 geolocations (Table 1, Fig. 1). Overall, data spanned 20–74° N and 57° W – 42° E, with individuals covering up to 45.2° in latitude ($\mu \pm \sigma$: 29.6 ± 9.0°) and 71.2° in longitude (45.6 ± 9.8°) with a maximal straight-line distance of up to 7122 km (3782 ± 1499 km) from the tagging location. Cumulative dis-

Table 1. Summary information for satellite-tagged *Cetorhinus maximus*. This includes shark ID, total body length (L_T), sex (M: male; F: female), location and date of tagging and pop-up, deployed tag types (PSAT: miniPAT-348; SPOT: SPOT6-253G), days at liberty (days between deployment and detachment [PSAT] and/or last high-quality position [SPOT; in parentheses]), days with SPOT-ARGOS positions, cumulative distance and days spent in either of the 3 high-use areas (H1−H3) based on most probable PSAT track, median and maximum (from minmax data; in parentheses) depth, median and range (in parentheses) of ambient temperature based on PSAT series data. Dates are given as d/mo/yr; Dash (−) indicates data not available

ID	Tagging date	L_T (m)	Sex	Tagging site	Tag type	Pop-up date	Pop-up site	Days at liberty	Days with SPOT loc.	Track dist. (km)	Occupancy (d)	Median (max) depth (m)	Median (Min−Max) temp. (°C)
B01[a]	30/06/2022	6.5±0.5	F	68.746 °N, 14.486 °E	PSAT	01/07/2023[e]	68.305° N, 12.82 8° E	366	−	13338	H1: 155, H2: 0, H3: 61	240 (1464)	8.8 (−0.5 to 16.8)
B02[a]	01/07/2022	5.5±0.5	−	68.216 °N, 15.000 °E	PSAT	02/07/2023[e]	55.704° N, 2.189° E	366	−	14441	H1: 91, H2: 0, H3: 0	29 (640)	7.6 (1.5−17.9)
B03	01/07/2022	7.5±0.5	F[d]	68.140 °N, 14.636 °E	PSAT	DNR	−	−	−	−	−	−	−
B04	17/06/2023	3.5±0.3	−	66.59° N, 12.652 °E	SPOT	−	−	(144)	84	−	−	−	−
B05	18/06/2023	7.5±0.3	M	67.57° N, 14.52° E	PSAT, SPOT	21/05/2024[f]	66.902° N, 2.997° E	338 (303)	5	16815	H1: 15, H2: 64, H3: 97	185 (989)	11.2 (0.2−18.7)
B06[a]	18/06/2023	7.3±0.3	F	67.53° N, 14.54° E	PSAT, SPOT	18/06/2024[e]	67.167° N, 12.23 5° E	366 (447)	42	12140	H1: 48, H2: 130, H3: 17	245 (1,400)	8.3 (−0.3 to 16.0)
B07	19/06/2023	8.4±0.5	M[d]	67.82° N, 13.64° E	SPOT	−	−	(515)	35	−	−	−	−
B08	20/06/2023	6.5±0.5	M	67.89° N, 13.66 ° E	PSAT, SPOT	15/03/2024[f]	46.555° N, 7.509° W	269 (343)	9	11085	H1: 29, H2: 22, H3: 135	213 (810)	12.2 (2.1−17.4)
B09[a]	20/06/2023	7.9±0.3	M	68.079° N, 14.015 ° E	PSAT	20/06/2024[e]	65.8° N, 10.7° E	366	−	13886	H1: 140, H2: 0, H3: 152	132 (1,392)	11.6 (−0.6 to 16.2)
B10	25/06/2023	7.6±0.3	F[d]	68.421° N, 14.015° E	PSAT	16/02/2024[e]	22.637° N, 56.629° W	236	−	8995	H1: 29, H2: 0, H3: 7	315 (976)	12.3 (0.2−27.4)
B11[b]	26/06/2023	8.3±0.3	F[d]	67.375° N, 14.215° E	PSAT	05/04/2024[g]	43.796° N, 29.619° W	284	−	7783	H1: 9, H2: 116, H3: 0	285 (600)	7.5 (7.0−15.9)
B12[b]	27/06/2023	8.1±0.3	M[d]	68.311° N, 14.945° E	PSAT	16/02/2024[e]	38.048° N, 11.201° W	234	−	7788	H1: 16, H2:129, H3: 19	298 (979)	7.8 (2.5−17.4)
B13[c]	01/07/2023	5.5±0.5	−	68.222° N, 14.576, ° E	PSAT	01/07/2024[e]	66.3° N, 11.4° E	366	−	−	−	−	−

[a]Available archive due to tag recovery, [b]Poor data transmission, [c]No data transmission, [d]Inferred from aerial footage
Release reasons: [e]Interval, [f]Tag failure (detached prematurely as it registered 'floating' even though it was still attached to the fish), [g]Too deep (DNR: did not report)

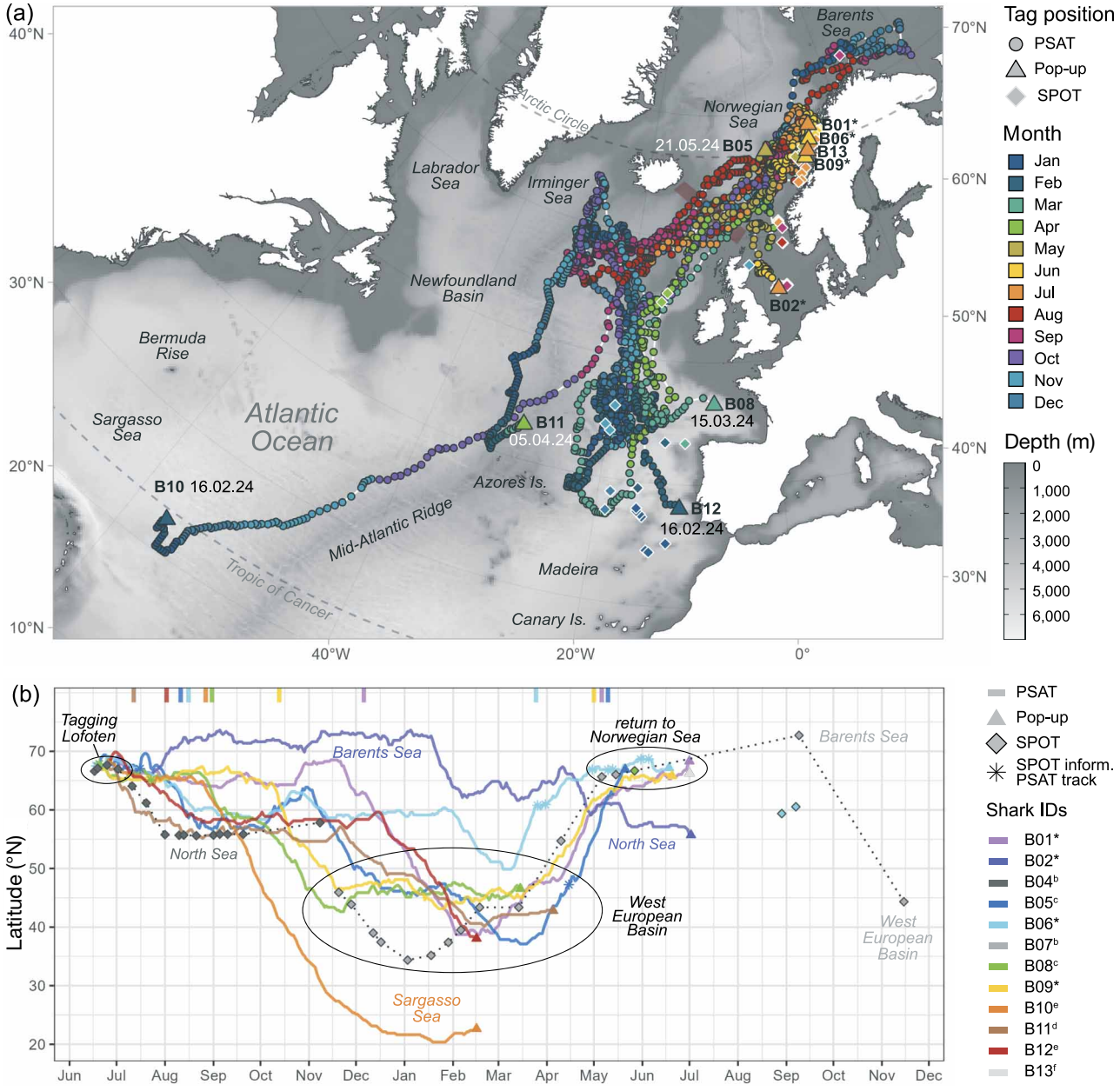

Fig. 1. Seasonality of horizontal movements based on *Cetorhinus maximus* tagged in June–July 2022 and 2023 with PSAT and SPOT tags in northern Norway (66.6–68.7° N). (a) Most probable daily positions of PSAT-tagged sharks (n = 9, points) and best daily numbered Argos locations not used for PSAT geolocation due to single tagging and/or transmission after pop-up date (4 sharks; diamonds) coloured by month. PSAT pop-up sites are shown as upward triangles together with shark ID and pop-up date for deployments <366 d. For individual tracks, Argos locations, and details of the Norwegian tagging and pop-up sites, see Figs. S3 & S5. (b) Latitudes of each PSAT track (line) or best weekly Argos location (asterisks: included in PSAT track; diamond: not included in PSAT track) over time following tagging, coloured by individual. Ticks on top mark crossings of the Iceland–Shetland Rise highlighted in (a) by the red polygon based on PSAT tracks. Associated with IDs, asterisks denote available archive due to tag recovery after 366 d, a: non-reporter, b: SPOT tag only, c: premature tag release (floater), d: premature tag release (too deep), e: programmed release on 16 February 2024, f: no data transmission

tances between tagging and pop-up locations ranged from 7783 to 16 815 km, with on average 14 124 ± 1729 km for sharks tagged ≥338 d. Average daily distances ranged from 27 to 50 km d^{-1} (37 ± 6 km d^{-1}). The 2 single SPOT-tagged individuals yielded 84 and 35 d with high-quality locations, covering 144 and 515 d at liberty, respectively. For B06 and B08, 3 and 1 additional high-quality location(s), respectively, were

recorded after PSAT deployment durations of 366 and 269 d (Table 1, Fig. 1b).

None of the 11 sharks with PSAT and/or SPOT data beyond tagging and pop-up information (excluding B03 and B13) remained exclusively in Norwegian waters across the deployment (Fig. 1; Figs. S3–S5). B02 and B07 moved north to the Barents Sea in late summer and autumn. Based on high-quality Argos positions, B07 was in the Barents Sea at 72.7° N, 25.2° E on 9 September 2024 (2nd year) before swimming more than 3900 km (straight-line distance) within 67 d to the West European Basin. Here, B07 was recorded in mid-November only 72 km northwest from where it had been detected 353 d earlier (Fig. 1; Figs. S4b & S5). Track reconstruction for B02 suggested that this shark resided in the Barents Sea from mid-August to early January, before moving south into the northern North Sea in spring (Fig. 1; Fig. S5). Its tag surfaced north of the Dogger Bank on 1 July 2023, at the same location that was utilized by B04 in August and September the following year (Fig. 1; Fig. S5).

Ten of 11 sharks with tracking data moved southwestwards from the tagging site, with most crossing the Greenland–Scotland Ridge via the Iceland–Faroe Rise or the Faroe–Shetland Channel in July and August (Fig. 1b). B09 and B01 resided in Norwegian waters until mid-October and early December, respectively, before moving south-westwards to the West European Basin and the Azores, without any occupation of the Iceland Basin in between. All sharks with post-summer southward movements and deployments ≥338 d (6 of 7, 86%) returned to the Northern Norwegian shelf the following spring, passing through the corridor between Iceland and Shetland from late March to early May (Fig. 1b). Including the pop-off location of B13, 7 of 8 sharks were recorded in Norwegian Sea and shelf waters 331–366 d after tagging, with respective pop-up and SPOT locations on average (μ ± σ) 246 ± 141 km from their original tagging site (Figs. S3b,c & S4). In the case of B07, whose tag remained active for 515 d, this annual movement pattern was repeated in the second year of deployment (Fig. 1b; Figs. S4b & S5).

Besides B10, all individuals remained east of 35° W in the NEA, and, with the exception of B11, east of the Mid-Atlantic Ridge. Between autumn and spring, most sharks resided in the oceanic waters of the Iceland and West European Basins between Iceland and the Azores, including members of both sexes. B11 seemed to have followed the Mid-Atlantic Ridge south to the Azores Plateau, where the tag detached in April after 284 d. B10 performed a transatlantic movement, covering 44° in latitude, 55° in longitude and 7,177 km cumulative distance between August and December before residing in the southern Sargasso Sea within the North American Basin from December to February, where the tag detached after 236 d ca. 760 km northeast of the West Indies. B10 and B11, the sharks that migrated the farthest based on straight-line distance from the tagging location, were among the largest individuals in the study and were presumed to be females based on their pectoral-fin markings.

3.2. Annual and seasonal high-use areas

The sharks occupied 3 main annual high-use areas in the NEA in which these individuals had likely spent 50% of the year. These included the Norwegian shelf and continental shelf break (H1) along Møre and Romsdal, Trøndelag, and Nordland including parts of the Vøring Plateau (0.2–8.5° E, 62.5–68.0° N), the Iceland Basin (H2) located southwest of Iceland between the Reykjanes Ridge and the Hatton-Rockall Plateau (33.1–20.2° W, 51.9–61.9° N), as well as the West European Basin (H3) between the Mid-Atlantic Ridge, Porcupine Bank, Bay of Biscay, and the Iberian Plain (26.4–13.6° W, 42.2–51.8° N; Fig. 2a). There was no evidence for extensive use of known summer 'hotspots' such as the shelf waters around the British Isles, including the Celtic Sea, Irish Sea, and Sea of the Hebrides.

There were clear seasonal differences in the utilization of H1–H3 (Fig. 2b–e; Figs. S6 & S7). H1 was primarily occupied during boreal summer between April and August. H2 was mainly utilized between September and November. While some individuals (B05, B06, B11, B12) showed elevated use of these waters, i.e. around the Reykjanes Ridge, others merely transited H2 (B08, B10) or utilized the neighbouring Hatton-Rockall Basin or Rockall Trough as the transit route to warm Atlantic waters (B01, B07, B09). H3 was predominantly used between December and March. Overall, August, December, and April were the main months in which sharks moved between high-use areas, despite notable variation in the timing and extent of these movements (Fig. 1).

3.3. Vertical distribution across habitats

Across the PSAT deployments, sharks utilized depths from the surface down to 1464 m and ambient temperatures from −0.6 to 27.4°C. Based on the daily histograms, sharks spent on average 40.7 ± 6.0% per day in waters in the top 150 m, of which 16.7 ± 2.3% was in the

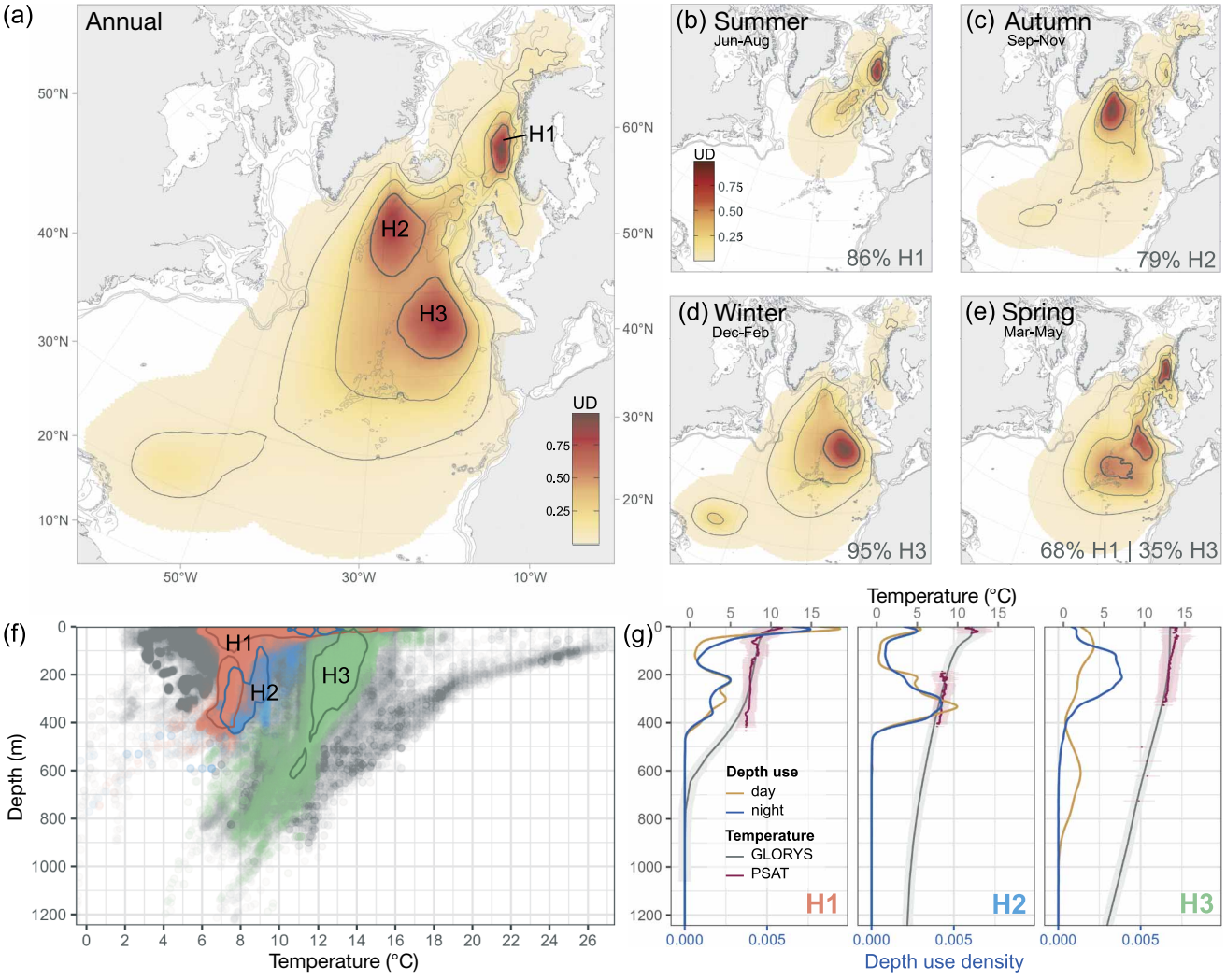

Fig. 2. High-use areas based on geolocated *Cetorhinus maximus* PSAT tracks (n = 9) and associated depth–temperature (DT) use from series data. (a) Annual and (b–e) seasonal utilization distributions (UDs) with isopleths marking the 50% (darker line), 75%, and 95% UD contours. Areas encompassed by the 50% UD contour in (a) delineate annual high-use areas (H1–H3). Percentage values in (b–e) indicate the proportion of the annual high-use area overlapping with the area enclosed by the seasonal 50% UD. For monthly UDs, see Fig. S6. (f) Occupied DT space (n = 253 499 data points; n = 13 expand beyond *y*-axis) with colours highlighting high-use area association and coloured lines denoting respective core DT envelopes (50% isoline). (g) Depth distribution as well as utilized and expected temperature profiles (mean ± SD) for each high-use area. Depth-use densities are shown for day (yellow) and night (blue), defined by sunset and sunrise at the most probable location (H1: n = 69 665, H2: n = 34 032; H3: n = 50 592). Tag-derived temperature profiles are shown in red (H1: n = 66 672, H2: n = 24 144; H3: n = 39 360). GLORYS-based temperature profiles for months of predominant use (H1: May–Jul, n = 8 sharks; H2: Sep–Nov, n = 6 sharks; H3: Jan–Mar, n = 6 sharks) are shown in grey

first 10 m (μ ± SE). More than half of the day (59.3 ± 6.0%) was spent between 150 and 1000 m. Here, the most frequented depth bins were 150–300 and 300–500 m, where sharks spent on average 28.3 ± 2.3 and 23.2 ± 5.1% of their time, respectively (Fig. S8a). Temperatures of 6–8°C were the most utilized (39.9 ± 7.1%), followed by 8–10, 10–12, and 12–14°C (16.8 ± 3.3, 14.6 ± 1.9, and 16.8 ± 4.5%, respectively; Fig. S8b).

We observed marked differences in the vertical shark distribution between high-use areas, particularly between the 2 northern (H1, H2) and the southern high-use area (H3). Both H1 and H2 were characterised by colder and more stratified waters, particularly pronounced in H1, in contrast to the warmer, thermally mixed water column of H3 (Fig. 2f,g).

In H1 and H2, sharks displayed bimodal depth use with elevated use of the upper 10 m (H1: 21.6 ± 4.0%; H2: 10.5 ± 5.0%) as well as depths between 150 and 500 m (H1: 55.2 ± 7.6%; H2: 71.1 ± 10.1%; Fig. S8c). At depth, sharks seemed to track particular isobaths

across both habitats (Fig. 3b; Fig. S9). Depths below 500 m were seldom frequented (H1: 0.1 ± 0.1%; H2: 0.3 ± 0.2%). While the water column was generally warmer in H2 ($H2_{z=0}$: 11.5°C; $H2_{z=200}$: 8.2°C) compared to H1 ($H1_{z=0}$: 10.5°C; $H1_{z=200}$: 7.5°C) differences in thermal habitat use were minor, with sharks predominantly utilizing waters of 6–8°C (H1: 66.5 ± 5.9%; H2: 57.7 ± 11.9%) in both high-use areas (Fig. S8d). This may be tied to sharks using surface waters only half as much in H2 and occupying deeper mesopelagic depth more than in H1. Unlike in H1, water below 4°C was rarely detected at mesopelagic depths in H2. In neither of the 2 areas did the sharks display large differences in depth use between day and night where a diel light regime was present (Fig. 2g).

This contrasted with depth and temperature use in H3. Here, the most frequented temperatures were 12–14°C (42.9 ± 10.1%) and while half of the time was spent at depths between 150 and 500 m (47.3 ± 3.4%), depths between 50 and 150 m and below 500 m were more frequented compared to H1 and H2 (Fig. 2f,g; Fig. S8c). The upper 10 m were used only 4.1 ± 1.1% of the time. A notable feature observed across individuals was the marked diel contrast in depths used within H3 and similar oceanic, lower-latitude waters in the North Atlantic (Figs. 2g & 3c). Strict nDVM behaviour with dusk ascents to depths between 100 and 300 m and dawn descents to greater mesopelagic depths was the most common pattern, but consistent phases of rDVM were also observed

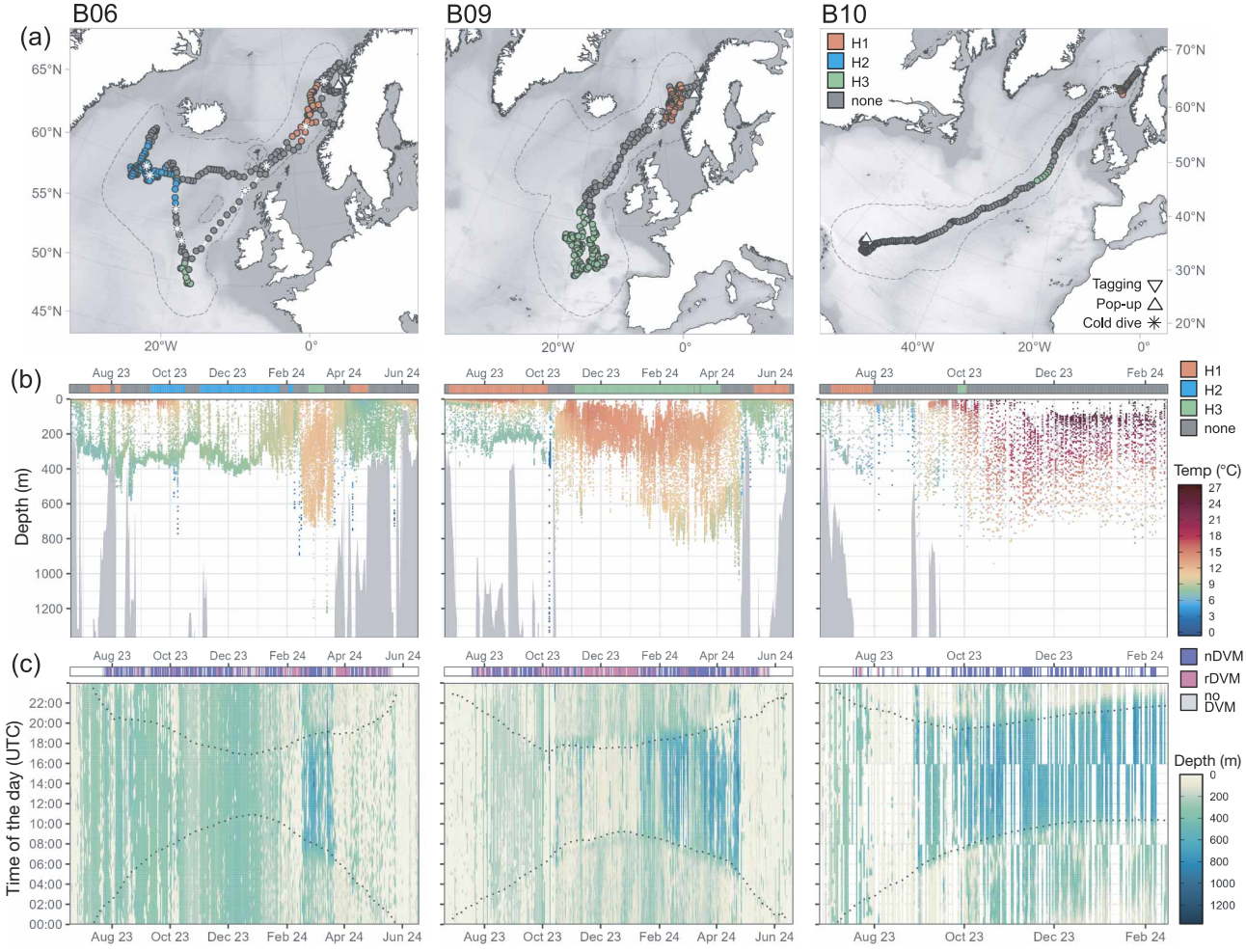

Fig. 3. Depth use behaviour of 3 *Cetorhinus maximus* across PSAT deployments. (a) Most probable tracks with daily positions coloured by their association to high-use areas. Asterisks denote locations where sharks performed cold-water (<3°C) dives beyond 400 m. Dashed lines show the 95% contour of the time integrated utilization distribution of each track. (b) Depth profiles coloured by temperature based on 10 min series from recovered (B06, n = 52 598; B09, n = 52 600) and transmitted (B10, n = 21 141) PSAT data. Local bathymetry for the most probable daily location is shown as grey polygons. Bar above highlights temporal association with high-use area. (c) Diel depth-use patterns with dotted lines indicating sunrise and sunset at the most probable location. Boreal summer was characterized by continuous daylight conditions. Bar above highlights days with significant diel vertical migration (DVM), with normal DVM shown in purple and reverse DVM in pink. Note that *x*-axis ranges vary across panels

between November and February (i.e. B05, B09), characterised by shallower epipelagic daytime depths (Fig. 3c; Fig. S10a). This shallower depth use in early winter also shaped individual differences in H3 of time spent below 500 m. While B05, B08, and B09, which arrived around November, spent only approximately 11% of their time below 500 m, B06 spent 26% and B01, B10, and B12 approximately 36% of time at these deeper mesopelagic depths.

Across all PSAT deployments, tracked sharks showed significant nDVM or rDVM behaviour for 32% (780 d) and 18% (439 d) of days, respectively. The remaining days were marked by no significant DVM (15%; 362 d) or did not have sufficient data or diel light regime to determine DVM behaviour (35%; 854 d). Contributions by individual and by high-use area are reported in Table S2 and Fig. S11, respectively.

Continuous display of nDVM behaviour was particularly evident in B10, which quickly transited H3 in late September following the Mid-Atlantic Ridge south-westwards past the Azores to the southern Sargasso Sea. Another notable feature in the depth distribution of this individual was its non-utilization of the first 90 m from mid-November onwards after entering waters southwest of 30° N and 46° W with SST around 26–27°C, which we consider indicative of surface-avoidance (Fig. 3b).

Inspection of the sharks' depth profiles, in conjunction with experienced temperatures and local bathymetry, revealed notable dives into cold waters (<3°C) before and after periods spent in warmer water environments, such as H3. These dives were observed in the Norwegian Basin, the Faroe–Shetland Channel (e.g. B01, B09). In the case of B06, the most probable track suggested cold-water dives occurred along the eastern fringes of the Iceland Basin; however, due to the limited east–west constraint of the input spatial likelihoods during this period, it is also possible that these dives took place in the western part of the adjacent Norwegian Basin (Fig. 3b; Fig. S9).

3.4. Large-scale latitudinal movements across seasonally fluctuating environments

Compared to lower-latitude sharks from Doherty et al. (2017a), high-latitude individuals in our study covered more than twice the latitudinal range and moved farther south on average. Lower-latitude individuals tagged around 56° N exhibited median monthly minimum latitudes ranging from 45.9 to 57.2° N (Δ11.3°) across the annual cycle. In contrast, high-latitude individuals tagged around 68° N ranged from 39.8 to 65.1° N (Δ25.3°) in their median minimum monthly latitude (Fig. 4a).

Movements of high-latitude individuals occurred in concert with seasonal latitudinal changes in SST and depth-integrated zooplankton biomass in the study area and study period. Mean monthly latitudes used by the sharks corresponded to an average median SST of 11.1 ± 2.1°C (μ ± σ), with high- and low-latitude bounds (μ ± σ) at 8.9 ± 1.3 and 15.2 ± 3.5°C, respectively (Fig. 4b). For zooplankton biomass, mean monthly shark latitudes corresponded to 2.1 ± 1.0 g m^{-2}, with high- and low-latitude bounds at 1.9 ± 0.9 and 1.8 ± 1.1 g m^{-2}, respectively (Fig. 4c). In spring, northward movements coincided with seasonal increases in temperature and secondary productivity above ~60° N and occurred substantially faster than the southward movements post-summer (Fig. 4b,c).

4. DISCUSSION

As the first long-term telemetry data set from the northernmost edge of the species' range, our results provide unique insights into the movement dynamics of and habitat use by *Cetorhinus maximus* in high-latitude environments, thereby broadening current understanding of its movement ecology across the North Atlantic.

4.1. Annual return migrations and inter-annual site fidelity

Repeated horizontal movements between boreal shelf habitats used in summer and lower-latitude offshelf habitats in winter suggest seasonal return migrations in these high-latitudinal individuals (Dingle 2014, Chapman et al. 2015). Ten of eleven sharks with sufficient data used both H1 and H3, and 7 of 8 sharks with ≥338 d deployments revisited H1 the following summer. Together with Argos positions showing repeated use of adjacent habitats, like the Barents and North Seas or the Faroe–Shetland Channel, and particularly the inter-annual use of both H1 and H3 by B07, these results provide evidence of regional philopatry and inter-annual site fidelity (sensu Chapman et al. 2015; acknowledging that natal and parturition sites remain unknown) in *C. maximus.* This is consistent with findings from other long-term telemetry, genetic analyses, and resightings at aggregation sites around the UK and Ireland (e.g. Sims et al. 2000, Gore et al. 2016, Doherty et al. 2017b, Dolton et al. 2020, Lieber et al. 2020, Thorburn et al. 2024). Such philopat-

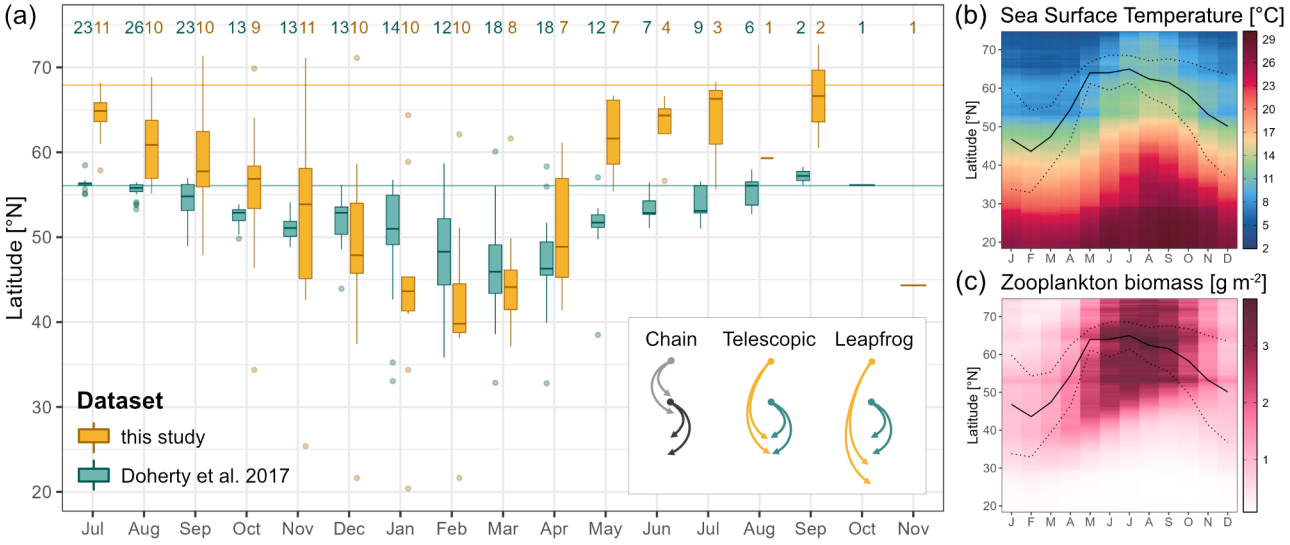

Fig. 4. Latitudinal movement cycle of high-latitude *Cetorhinus maximus*. (a) Minimum monthly latitudes from PSAT and SPOT data in this study, compared with those reported by Doherty et al. (2017a) for *C. maximus* tagged off the west coast of Scotland and the Isle of Man. Boxes represent the median and interquartile range (IQR), whiskers extend to 1.5× IQR, and outliers are shown as points. The number of contributing individuals is indicated above each box, and horizontal lines denote the mean latitude of summer tagging locations for both studies. Inset shows conceptual illustration of the 3 main latitudinal migration patterns based on Chapman et al. (2014), with colours highlighting the patterns reflected in the presented datasets. (b,c) Average monthly latitude (mean ± SD) of high-latitude individuals (n = 12) in relation to monthly climatologies of sea surface temperature and zooplankton biomass (in carbon; 0–1000 m) within the study area and period

ric behaviour, also documented in other elasmobranchs including the closely related family of mackerel sharks (Jorgensen et al. 2010, Saunders et al. 2025), suggests that *C. maximus* possesses the necessary sensory and cognitive capacities to reliably orientate and/or navigate dynamic marine environments (Montgomery & Walker 2001, Keller et al. 2021).

Averaging over 14 000 km annually, these large-scale movements are among the longest seasonal migrations recorded for sharks (e.g. Bonfil et al. 2005, Sequeira et al. 2013, Queiroz et al. 2019). While we observed plasticity with regards to the timing of southward movements post-summer (i.e. passing the Greenland–Shetland Rise), the exact location of winter residency areas (i.e. West European Basin, Mid-Atlantic Ridge, southern Sargasso Sea), the duration of time spent there (weeks to months), and likely the individual routes taken, observed latitudinal movements were relatively consistent in their seasonal sequence and large latitudinal extent.

The migration sequence of moving to higher latitudes along continental shelf edges in a confined time window between late March and early May aligns with the northward progression of secondary productivity (Planque & Batten 2000) and is consistent with early theories of *C. maximus* movements in the NEA, suggesting north–south and west–east migration based on historical records from Scotland and Ireland (Sims 2008) and the historical Norwegian *C. maximus* fishery (Aasen 1966, Stott 1982). Post-summer movements off the shelf and/or to lower latitudes correspond to patterns documented for *C. maximus* in the NWA (Skomal et al. 2004, Braun et al. 2018b) and NEP (Dewar et al. 2018) and align with sightings and tracking data along the Iberian and Moroccan coasts between January and May (Couto et al. 2017, Doherty et al. 2017a, Dolton et al. 2020). Similar seasonal migration sequences have also been observed in other marine megafauna (e.g. Block et al. 2011, Vaudo et al. 2017, Franks et al. 2021, Kettemer et al. 2022, Ferter et al. 2024).

With all PSAT tracks leaving the Norwegian Sea and covering on average 30 ± 9° in latitude, observed latitudinal movements were consistently extensive, akin to ranges reported for *C. maximus* tagged off New England (Skomal et al. 2009, Braun et al. 2018b). This contrasts with the more variable small- to medium-scale movement patterns reported for lower-latitude individuals with summer residency in known 'hotspots' like the Celtic Sea, Irish Sea, or Sea of the Hebrides (Sims et al. 2003, Doherty et al. 2017a, Dolton et al. 2020, Johnston et al. 2022). Well-documented in birds (e.g. Duijns et al. 2012, Ramos et al. 2015) and increasingly recognised in other taxa (e.g. Singh et al. 2012, Geijer et al. 2016), including sharks

(e.g. Lubitz et al. 2022, Niella et al. 2022), individuals with summer occupancy at the high-latitudinal edge of the distribution often undertake longer and less variable seasonal movements than those within the centre of the distribution. Such dynamics can result in telescopic or leapfrog migrations, in which high-latitude individuals bypass central high-use areas and migrate to similar (telescopic) or lower (leapfrog) latitudes than lower-latitude conspecifics — contrasting with chain migration, where peripheral and central individuals migrate over comparable latitudinal extents (Lundberg & Alerstam 1986). Consistent with this framework, high-latitude *C. maximus* in our study on average covered more than twice the latitudinal range of lower-latitude individuals tracked by Doherty et al. (2017a), bypassing shelf-based summer aggregation sites and moving to similar or more southern overwintering areas, providing first evidence for both telescopic and leapfrog migration in the NEA.

Such differences in movement behaviour between high- and lower-latitude individuals indicate marked intra-specific variation in horizontal movements within the NEA. Combined with the evidence for high inter-annual site fidelity corroborated by this study, this variability likely affects population structure (Chapman et al. 2015). First evidence of genetic distinctions between migratory sharks off southwest Ireland in spring and those found later in the season in the Sea of the Hebrides and Irish Sea, along with the higher relatedness among co-occurring individuals identified by Lieber et al. (2020), provide initial support for potential population structuring within the NEA.

However, while regional philopatry appears common in *C. maximus* based on this and previous studies, incidental records indicate that inter-annual fidelity to summer residence areas may not be obligate nor necessarily exhibited by all individuals. For instance, a male tracked by Dolton et al. (2020) shifted its summer use from the Irish Sea to the Norwegian Sea in consecutive years, following a route through the West European Basin and Faroe–Shetland Channel similar to individuals in our study. Likewise, a female tagged off Ireland in August was re-sighted off Massachusetts (USA) in summer 3 yr later (Johnston et al. 2019). Such inter-annual site switching, together with far-ranging, possibly female-biased movements (Gore et al. 2008, Skomal et al. 2009, Braun et al. 2018b, Johnston et al. 2019, this study), and the observed plasticity in post-summer migration timing, duration, and destination, likely contribute to maintaining population connectivity. Long-term (≥1 yr) telemetry, combined with expanded genetic sampling across summer aggregation sites, will be critical for quantifying individual- and population-level plasticity in movement strategies and for developing a more comprehensive understanding of population structure and connectivity within the NEA and across the wider North Atlantic.

4.2. Seasonal residency and habitat use

Tracked *C. maximus* displayed marked seasonal residency (sensu Chapman et al. 2015), occupying Norwegian Sea shelf and shelf-edge habitats between April and August (H1), and the West European Basin and adjacent regions between December and March (H3). H1 aligns with historic *C. maximus* fishing grounds (Stott 1982) and more recent summer records from Norway (Mecklenburg et al. 2018), whereas H3 corresponds to winter sightings and tag-based observations of *C. maximus* (Couto et al. 2017, Doherty et al. 2017a, Dolton et al. 2020, Johnston et al. 2022), and overlaps with high-use areas of other marine predators, including Atlantic bluefin tuna *Thunnus thynnus* (Pagniello et al. 2023, Ferter et al. 2024) and blue sharks *Prionace glauca* (Vandeperre et al. 2014, Queiroz et al. 2019). The Icelandic Basin, which, like the Norwegian and Barents Seas, is highly productive and supports important feeding grounds for planktivorous megafauna (Sigurjónsson & Víkingsson 1997, García-Vernet et al. 2021, IUCN SSC Shark Specialist Group 2024), was used between September and November, albeit less consistently and with greater geolocation uncertainty than the other high-use areas.

Vertically, boreal shelf habitats were characterised by irregular surface use and isobath tracking, with surface use declining towards autumn, whereas at lower latitudes, isothermic oceanic waters were dominated by mesopelagic occupancy and DVM during winter. These patterns are consistent with depth use recorded in the NEA (Doherty et al. 2019, Johnston et al. 2022), NWA (Braun et al. 2018b, 2023), and NEP (Dewar et al. 2018), and align with the known vertical distributions of zooplanktonic prey in the Norwegian Sea (Røstad et al. 2016, Aarflot et al. 2019, Chamorro et al. 2025) and the warm-temperate waters of the NEA (Peña et al. 2020, García-Seoane et al. 2023, Diogoul et al. 2026), as detailed by Klöcker et al. (2025a). Collectively, this indicates that *C. maximus* vertically tracks its prey across habitats year-round.

Ambient temperature data from high-latitude individuals show that previous studies had not yet captured the lower tolerance limit of the species (Klöcker et al. 2025a, this study). With a thermal tolerance spanning roughly 30°C (−0.6 to 27.4°C, this study; 4.2

to 29.9°C, Braun et al. 2018b), *C. maximus* appears less thermally constrained than most other sharks (e.g. Lear et al. 2019), likely facilitated by its large thermal inertia and anatomical adaptations that reduce heat loss (Klöcker et al. 2025b). Nevertheless, at distributional edges, where sharks are presumably exposed to their thermal limits, behavioural signs of thermal constraint become evident. In the Norwegian and Barents Seas, lipid-rich *Calanus* spp. that constitute a key component of the diet of *C. maximus* (Sims & Merrett 1997, Sims 1999) are associated with waters <1°C upon entering diapause in late summer (Gaardsted et al. 2010, Daase et al. 2021, Gawinski et al. 2024). Although *C. maximus* can tolerate brief exposures to temperatures ≤2°C during dives, our data indicate that the sharks do not remain in such cold waters for more than a few hours, nor do they venture north of the polar front to access these high-quality prey resources (this study; Klöcker et al. 2025a). Conversely, when encountering sea surface temperatures >25°C at low latitudes, B11 exhibited surface-avoidance behaviour, consistent with Braun et al. (2018b), seemingly allowing this cold-adapted species to traverse tropical regions without prolonged exposure to temperatures outside its thermal preference limits (Skomal et al. 2009, Braun et al. 2018b). Collectively, these findings suggest that *C. maximus* is relatively unconstrained by water temperatures between approximately 2 and 25°C, a range that encompasses most of its core distribution, including the epi- and upper mesopelagic zones of the Norwegian Sea throughout the year.

4.3. Potential drivers of latitudinal migration

Considering recorded eurythermy and apparent year-round tracking of vertical prey layers, repeated large-scale horizontal movements and leapfrog patterns observed in high-latitude individuals are most plausibly linked to seasonal oscillations in prey availability (Sims & Reid 2002, Alò et al. 2021). Boreal waters supply exceptionally energy-rich zooplanktonic prey for migratory filter-feeders during short productivity windows in summer (Falk-Petersen et al. 2009, Daase et al. 2021), likely providing an energetic surplus for *C. maximus* in these habitats. However, post-summer access to these boreal prey resources may be constrained as waters in the lower mesopelagic and at higher latitudes approach the species' thermal limits for prolonged use, while shallower depth layers in the Norwegian Sea may offer insufficient zooplankton biomass to meet the energetic demands of these obligate ram filter feeders. Thus, seasonal migrations in these high latitude individuals likely reflect prey-driven responses shaped both directly by the sharks' thermal preferences at the range edge and indirectly by environmentally mediated changes in prey distribution, which amplify with latitude.

Southward movements to deep, isothermic waters in subtropical gyres may also serve reproductive functions, as proposed for whales (Lockyer & Brown 1981, Corkeron & Connor 1999) and closely related lamnid sharks (e.g. Gilmore 1993, Weng et al. 2008, Campana et al. 2010, Franks et al. 2021). While both sexes equally used the West European Basin, sporadic records (Gore et al. 2008, Skomal et al. 2009, Braun et al. 2018b, Johnston et al. 2019, this study) may suggest that mature females undertake particularly wide-ranging movements, potentially explaining the scarcity in observations of pregnant *C. maximus* and young-of-the-year in mid- to high-latitude coastal waters (Sims 2008). Nonetheless, the role of reproduction in these large-scale movements remains unresolved, highlighting the need for long-term, year-round tracking across demographic groups and improved understanding of the reproductive biology of *C. maximus*.

5. CONCLUDING REMARKS

Our study demonstrates that incorporating high-latitude individuals is essential for a comprehensive understanding of movement ecology in marine megafauna, revealing patterns that would otherwise remain undetected. Year-round tracking of high-latitude individuals of *Cetorhinus maximus* in the North Atlantic revealed some of the longest seasonal return movements recorded for any shark species (~14 000 km annually) and one of the broadest thermal tolerances (~30°C), enabling sustained, active habitat use from subpolar to subtropical waters. Compared with lower-latitude individuals from previous studies, these high-latitude sharks made consistent, large-scale southward movements in a 'leapfrog' pattern, likely reflecting the influence of pronounced seasonal resource fluctuations at these latitudes and revealing considerable intra-specific variability in horizontal movement behaviour in the NEA.

Despite their high mobility, the seasonal residency and inter-annual site fidelity observed in *C. maximus* underscore the value of spatio-temporally explicit management of key habitats, such as the Norwegian Shelf and migration corridors like the Iceland–Shetland Rise, which are also important for other migratory megafauna (e.g. Lydersen et al. 2020, Ket-

temer et al. 2022, Bortoluzzi et al. 2024, Ferter et al. 2024, Lydersen et al. 2025). In the context of rapid Atlantification of the Arctic (Ingvaldsen et al. 2021, Freer et al. 2022, Gerland et al. 2023) and increasing vertical habitat compression from warming surface waters and expanding oxygen minimum zones at lower latitudes (Waller et al. 2024), dynamic management approaches that anticipate shifts in distribution and phenology will be essential for highly mobile species like *C. maximus*, particularly at the range edges. Future integration of behavioural, physiological, and genetic data across latitudes will be instrumental to elucidate the mechanisms underlying these annual movements and informing effective conservation strategies under accelerating climate change.

Acknowledgements. The study was financed by the Research Council of Norway via the Sharks on the Move project (RCN #326879) and forms part of C.A.K.'s PhD thesis. M.C.A. was supported by the Woods Hole Oceanographic Institution (WHOI) President's Innovation Fund. P.L. was supported by the European Union (MARHAB, grant no. 101135307). N.Q. was funded by Fundação para a Ciência e a Tecnologia (FCT) through grant CEECIND/02857/2018. D.W.S. was supported by a European Research Council Advanced Grant (ERC-AdG-883583 OCEAN DEOXYFISH). We acknowledge Ingrid M. Bruvold (Havforskningsinstituttet) as well as the Norwegian coast guard and the Norwegian Directorate of Fisheries for facilitating the fieldwork and tag recovery. Special thanks to Marisa Vedor (CIBIO) for her assistance in data handling. Further, we thank the Shark Trust for their collaboration in developing outreach materials as well as the public for reporting sightings, which have been instrumental in this work. Tagging and sampling procedures were approved by the Norwegian Food Safety Authority (FOTS ID 29672). P.I.M. acknowledges NERC Earth Observation Data Analysis and Artificial-Intelligence Service (NEODAAS) for the use of computing resources.

LITERATURE CITED

Aarflot JM, Aksnes DL, Opdal AF, Skjoldal HR, Fiksen Ø (2019) Caught in broad daylight: topographic constraints of zooplankton depth distributions. Limnol Oceanogr 64: 849–859

Aasen O (1966) Brugde, *Cetorhinus maximus* (Gunnerus), 1765. Fiskets Gang (Fish Rev) 49:909–920

Alò D, Lacy SN, Castillo A, Samaniego HA, Marquet PA (2021) The macroecology of fish migration. Glob Ecol Biogeogr 30:99–116

Andrzejaczek S, Lucas TCD, Goodman MC, Hussey NE and others (2022) Diving into the vertical dimension of elasmobranch movement ecology. Sci Adv 8:eabo1754

Arostegui MC, Afonso P, Fauconnet L, Fontes J and others (2024) Advancing the frontier of fish geolocation into the ocean's midwaters. Deep Sea Res I 212:104386

Banzon V, Smith TM, Chin TM, Liu C, Hankins W (2016) A long-term record of blended satellite and in situ sea-surface temperature for climate monitoring, modeling and environmental studies. Earth Syst Sci Data 8:165–176

Becker JJ, Sandwell DT, Smith WHF, Braud J and others (2009) Global bathymetry and elevation data at 30 arc seconds resolution: SRTM30_PLUS. Mar Geod 32:355–371

Béguer-Pon M, Benchetrit J, Castonguay M, Aarestrup K, Campana SE, Stokesbury MJW, Dodson JJ (2012) Shark predation on migrating adult American eels (*Anguilla rostrata*) in the Gulf of St. Lawrence. PLOS ONE 7:e46830

Block BA, Jonsen ID, Jorgensen SJ, Winship AJ and others (2011) Tracking apex marine predator movements in a dynamic ocean. Nature 475:86–90

Bonfil R, Meÿer M, Scholl MC, Johnson R and others (2005) Transoceanic migration, spatial dynamics, and population linkages of white sharks. Science 310:100–103

Bortoluzzi JR, McNicholas GE, Jackson AL, Klöcker CA and others (2024) Transboundary movements of porbeagle sharks support need for continued cooperative research and management approaches. Fish Res 275:107007

Braun CD, Galuardi B, Thorrold SR (2018a) HMMoce: an R package for improved geolocation of archival-tagged fishes using a hidden Markov method. Methods Ecol Evol 9:1212–1220

Braun CD, Skomal GB, Thorrold SR (2018b) Integrating archival tag data and a high-resolution oceanographic model to estimate basking shark (*Cetorhinus maximus*) movements in the Western Atlantic. Front Mar Sci 5:25

Braun CD, Della Penna A, Arostegui MC, Afonso P and others (2023) Linking vertical movements of large pelagic predators with distribution patterns of biomass in the open ocean. Proc Natl Acad Sci USA 120:e2306357120

Byrd RH, Lu P, Nocedal J, Zhu C (1995) A limited memory algorithm for bound constrained optimization. SIAM J Sci Comput 16:1190–1208

Campana S, Joyce W, Fowler G (2010) Subtropical pupping ground for a cold-water shark. Can J Fish Aquat Sci 67: 769–773

Chamorro E, Ellingsen I, Broch OJ, Weidberg N, Basedow SL (2025) Variability of *Calanus* spp. spatial aggregations in the subarctic shelf and oceanic region using *in-situ* data and the coupled biophysical ocean model SINMOD. ICES J Mar Sci 82:fsaf174

Chapman BB, Skov C, Hulthén K, Brodersen J, Nilsson PA, Hansson LA, Brönmark C (2012) Partial migration in fishes: definitions, methodologies and taxonomic distribution. J Fish Biol 81:479–499

Chapman BB, Eriksen A, Baktoft H, Brodersen J and others (2013) A foraging cost of migration for a partially migratory cyprinid fish. PLOS ONE 8:e61223

Chapman B, Hulthén K, Wellenreuther M, Hansson LA, Nilsson JA, Brönmark C (2014) Patterns of animal migration. In: Hansson LA, Åkesson S (eds) Animal movement across scales. Oxford University Press, New York, NY, p 11–35

Chapman DD, Feldheim KA, Papastamatiou YP, Hueter RE (2015) There and back again: a review of residency and return migrations in sharks, with implications for population structure and management. Annu Rev Mar Sci 7: 547–570

CMEMS (Copernicus Marine Environment Monitoring Service) (2024a) Global ocean low and mid trophic levels biomass content hindcast. https://data.marine.copernicus.eu/product/GLOBAL_MULTIYEAR_BGC_001_033/description

CMEMS (2024b) Global Ocean Physics Reanalysis. https://data.marine.copernicus.eu/product/GLOBAL_MULTIYEAR_PHY_001_030/description

Corkeron PJ, Connor RC (1999) Why do baleen whales migrate? Mar Mamm Sci 15:1228–1245

Couto A, Queiroz N, Relvas P, Baptista M and others (2017) Occurrence of basking shark *Cetorhinus maximus* in

southern Portuguese waters: a two-decade survey. Mar Ecol Prog Ser 564:77–86

Daase M, Berge J, Søreide JE, Falk-Petersen S (2021) Ecology of Arctic pelagic communities. In: Thomas DN (ed) Arctic ecology. John Wiley & Sons, Oxford, p 219–259

Dewar H, Wilson SG, Hyde JR, Snodgrass OE and others (2018) Basking shark (*Cetorhinus maximus*) movements in the eastern North Pacific Determined using satellite telemetry. Front Mar Sci 5:163

Dingle H (2014) Migration: the biology of life on the move, 2nd edn. Oxford University Press, New York, NY

Diogoul N, Brehmer P, Jouanno J, Perrot Y and others (2026) Characterisation of pelagic seascapes through micronektonic and zooplanktonic scattering layers. Sci Rep 16: 6378

Doherty PD, Baxter JM, Gell FR, Godley BJ and others (2017a) Long-term satellite tracking reveals variable seasonal migration strategies of basking sharks in the north-east Atlantic. Sci Rep 7:42837

Doherty PD, Baxter JM, Godley BJ, Graham RT and others (2017b) Testing the boundaries: seasonal residency and inter-annual site fidelity of basking sharks in a proposed Marine Protected Area. Biol Conserv 209:68–75

Doherty PD, Baxter JM, Godley BJ, Graham RT and others (2019) Seasonal changes in basking shark vertical space use in the north-east Atlantic. Mar Biol 166:129

Dolton HR, Gell FR, Hall J, Hall G, Hawkes LA, Witt MJ (2020) Assessing the importance of Isle of Man waters for the basking shark *Cetorhinus maximus.* Endang Species Res 41:209–223

Douglas DC, Weinzierl RC, Davidson S, Kays R, Wikelski M, Bohrer G (2012) Moderating Argos location errors in animal tracking data. Methods Ecol Evol 3:999–1007

Duijns S, Jukema J, Spaans B, van Horssen P, Piersma T (2012) Revisiting the proposed leap-frog migration of bar-tailed godwits along the East-Atlantic flyway. Ardea 100:37–43

Falk-Petersen S, Mayzaud P, Kattner G, Sargent JR (2009) Lipids and life strategy of Arctic *Calanus*. Mar Biol Res 5: 18–39

Ferter K, Pagniello CMLS, Block BA, Bjelland O and others (2024) Atlantic bluefin tuna tagged off Norway show extensive annual migrations, high site-fidelity and dynamic behaviour in the Atlantic Ocean and Mediterranean Sea. Proc R Soc B 291:20241501

Franks BR, Tyminski JP, Hussey NE, Braun CD and others (2021) Spatio-temporal variability in white shark (*Carcharodon carcharias*) movement ecology during residency and migration phases in the western North Atlantic. Front Mar Sci 8:744202

Freer JJ, Daase M, Tarling GA (2022) Modelling the biogeographic boundary shift of *Calanus finmarchicus* reveals drivers of Arctic Atlantification by subarctic zooplankton. Glob Change Biol 28:429–440

Gaardsted F, Zhou M, Pavlov V, Morozov A, Tande KS (2010) Mesoscale distribution and advection of overwintering *Calanus finmarchicus* off the shelf of northern Norway. Deep Sea Res I 57:1465–1473

García-Seoane E, Klevjer T, Mork KA, Agersted MD, Macaulay GJ, Melle W (2023) Acoustic micronektonic distribution and density is structured by macroscale oceanographic processes across 17–48° N latitudes in the North Atlantic Ocean. Sci Rep 13:4614

García-Vernet R, Borrell A, Víkingsson G, Halldórsson SD, Aguilar A (2021) Ecological niche partitioning between baleen whales inhabiting Icelandic waters. Prog Oceanogr 199:102690

Gawinski C, Basedow SL, Sundfjord A, Svensen C (2024) Secondary production at the Barents Sea polar front in summer: contribution of different size classes of mesozooplankton. Mar Ecol Prog Ser 735:77–101

GEBCO Compilation Group (2023) GEBCO 2023 Grid. https://www.gebco.net/data-products/gridded-bathymetry-data/gebco2023-grid

Geijer CKA, Notarbartolo di Sciara G, Panigada S (2016) Mysticete migration revisited: Are Mediterranean fin whales an anomaly? Mammal Rev 46:284–296

Gerland S, Ingvaldsen RB, Reigstad M, Sundfjord A and others (2023) Still Arctic? — The changing Barents Sea. Elementa Sci Anthropocene 11:00088

Gilmore RG (1993) Reproductive biology of lamnoid sharks. Environ Biol Fishes 38:95–114

Gore MA, Rowat D, Hall J, Gell FR, Ormond RF (2008) Transatlantic migration and deep mid-ocean diving by basking shark. Biol Lett 4:395–398

Gore MA, Frey PH, Ormond RF, Allan H, Gilkes G (2016) Use of photo-identification and mark–recapture methodology to assess basking shark (*Cetorhinus maximus*) populations. PLOS ONE 11:e0150160

Hijmans RJ (2024) geosphere: spherical trigonometry. R package version 1.5-20. https://CRAN.R-project.org/web/packages/geosphere/

Hill RD, Braun MJ (2001) Geolocation by light level. In: Sibert JR, Nielsen JL (eds) Electronic tagging and tracking in marine fisheries: Proceedings of the Symposium on Tagging and Tracking Marine Fish with Electronic Devices, East-West Center, University of Hawaii, 7–11 February 2000. Springer, Dordrecht, p 315–330

Hueter RE, Heupel MR, Heist EJ, Keeney DB (2005) Evidence of philopatry in sharks and implications for the management of shark fisheries. J Northwest Atl Fish Sci 35:239–247

Ingvaldsen RB, Assmann KM, Primicerio R, Fossheim M, Polyakov IV, Dolgov AV (2021) Physical manifestations and ecological implications of Arctic Atlantification. Nat Rev Earth Environ 2:874–889

IUCN SSC Shark Specialist Group (2024) Faxaflói Bay ISRA Factsheet. IUCN SSC Shark Specialist Group, Dubai

Johnston EM, Mayo PA, Mensink PJ, Savetsky E, Houghton JDR (2019) Serendipitous re-sighting of a basking shark *Cetorhinus maximus* reveals inter-annual connectivity between American and European coastal hotspots. J Fish Biol 95:1530–1534

Johnston EM, Houghton JDR, Mayo PA, Hatten GKF, Klimley AP, Mensink PJ (2022) Cool runnings: behavioural plasticity and the realised thermal niche of basking sharks. Environ Biol Fishes 105:2001–2015

Jorgensen SJ, Reeb CA, Chapple TK, Anderson S and others (2010) Philopatry and migration of Pacific white sharks. Proc R Soc B 277:679–688

Keller BA, Putman NF, Grubbs RD, Portnoy DS, Murphy TP (2021) Map-like use of Earth's magnetic field in sharks. Curr Biol 31:2881–2886.e3

Kettemer LE, Rikardsen AH, Biuw M, Broms F, Mul E, Blanchet MA (2022) Round-trip migration and energy budget of a breeding female humpback whale in the Northeast Atlantic. PLOS ONE 17:e0268355

Klöcker CA, Bjelland O, Ferter K, Arostegui MC and others (2025a) Basking sharks of the Arctic Circle: year-long, high-resolution tracking data reveal wide thermal range and prey-driven vertical movements across habitats. Anim Biotelem 13:15

Klöcker CA, Schlindwein A, Arostegui MC, Bruvold IM and others (2025b) Giants in the cold: morphological evi-

dence for vascular heat retention in the viscera but not the skeletal muscle of the basking shark (*Cetorhinus maximus*). J Fish Biol, https://doi.org/10.1111/jfb.70052
Lear KO, Whitney NM, Morgan DL, Brewster LR and others (2019) Thermal performance responses in free-ranging elasmobranchs depend on habitat use and body size. Oecologia 191:829–842
Lehodey P, Murtugudde R, Senina I (2010) Bridging the gap from ocean models to population dynamics of large marine predators: a model of mid-trophic functional groups. Prog Oceanogr 84:69–84
Lehodey P, Conchon A, Senina I, Domokos R and others (2015) Optimization of a micronekton model with acoustic data. ICES J Mar Sci 72:1399–1412
Lellouche JM, Greiner E, Le Galloudec O, Garric G and others (2018) Recent updates to the Copernicus Marine Service global ocean monitoring and forecasting real-time 1/12° high-resolution system. Ocean Sci 14:1093–1126
Lieber L, Hall G, Hall J, Berrow S and others (2020) Spatio-temporal genetic tagging of a cosmopolitan planktivorous shark provides insight to gene flow, temporal variation and site-specific re-encounters. Sci Rep 10:1661
Lien J, Lien J, Fawcett L (1986) Distribution of basking sharks, *Cetorhinus maximus*, incidentally caught in inshore fishing gear in Newfoundland. Can Field Nat 100:246–252
Lockyer CH, Brown SG (1981) The migration of whales. In: Aidley DJ (ed) Animal migration. Cambridge University Press, New York, NY, p 105–137
Lubitz N, Bradley M, Sheaves M, Hammerschlag N, Daly R, Barnett A (2022) The role of context in elucidating drivers of animal movement. Ecol Evol 12:e9128
Lundberg S, Alerstam T (1986) Bird migration patterns: conditions for stable geographical population segregation. J Theor Biol 123:403–414
Luo J, Ault JS, Shay LK, Hoolihan JP, Prince ED, Brown CA, Rooker JR (2015) Ocean heat content reveals secrets of fish migrations. PLOS ONE 10:e0141101
Lydersen C, Vacquié-Garcia J, Heide-Jørgensen MP, Øien N, Guinet C, Kovacs KM (2020) Autumn movements of fin whales (*Balaenoptera physalus*) from Svalbard, Norway, revealed by satellite tracking. Sci Rep 10:16966
Lydersen C, Blanchet MA, Kovacs KM, Similä T and others (2025) Migration to breeding areas by male sperm whales *Physeter macrocephalus* from the Northeast Atlantic Arctic. Sci Rep 15:7861
McMillan MN, Huveneers C, Semmens JM, Gillanders BM (2019) Partial female migration and cool-water migration pathways in an overfished shark. ICES J Mar Sci 76: 1083–1093
Mecklenburg CW, Lynghammar A, Johannesen E, Byrkjedal I and others (2018) Marine fishes of the Arctic region, Vol 2. Conservation of Arctic flora and fauna (CAFF) Monitoring Series Report 28. CAFF, Akureyri
Miller PI, Scales KL, Ingram SN, Southall EJ, Sims DW (2015) Basking sharks and oceanographic fronts: quantifying associations in the north-east Atlantic. Funct Ecol 29:1099–1109
Montgomery JC, Walker MM (2001) Orientation and navigation in elasmobranchs: which way forward? Environ Biol Fishes 60:109–116
Niella Y, Butcher P, Holmes B, Barnett A, Harcourt R (2022) Forecasting intraspecific changes in distribution of a wide-ranging marine predator under climate change. Oecologia 198:111–124
Nielsen JK, Bryan DR, Rand KM, Arostegui MC, Braun CD, Galuardi B, McDermott SF (2023) Geolocation of a demersal fish (Pacific cod) in a high-latitude island chain (Aleutian Islands, Alaska). Anim Biotelem 11:29
Nyegaard M, Braun CD, Welly M, Djohani R, Arostegui MC (2023) Overcoming challenging telemetry data of giant sunfish *Mola alexandrini* (Molidae) in Bali, Indonesia. Mar Ecol Prog Ser 722:157–175
Pagniello CMLS, Ó'Maoiléidigh N, Maxwell H, Castleton MR and others (2023) Tagging of Atlantic bluefin tuna off Ireland reveals use of distinct oceanographic hotspots. Prog Oceanogr 219:103135
Papastamatiou YP, Meyer CG, Carvalho F, Dale JJ, Hutchinson MR, Holland KN (2013) Telemetry and random-walk models reveal complex patterns of partial migration in a large marine predator. Ecology 94:2595–2606
Peña M, Cabrera-Gámez J, Domínguez-Brito AC (2020) Multi-frequency and light-avoiding characteristics of deep acoustic layers in the North Atlantic. Mar Environ Res 154:104842
Planque B, Batten SD (2000) *Calanus finmarchicus* in the North Atlantic: the year of *Calanus* in the context of interdecadal change. ICES J Mar Sci 57:1528–1535
Powell RA, Mitchell MS (2012) What is a home range? J Mammal 93:948–958
Queiroz N, Humphries NE, Couto A, Vedor M and others (2019) Global spatial risk assessment of sharks under the footprint of fisheries. Nature 572:461–466
R Core Team (2023) R: a language and environment for statistical computing. R Foundation for Statistical Computing, Vienna
Ramos R, Sanz V, Militão T, Bried J and others (2015) Leap-frog migration and habitat preferences of a small oceanic seabird, Bulwer's petrel (*Bulweria bulwerii*). J Biogeogr 42:1651–1664
Reynolds RW, Smith TM, Liu C, Chelton DB, Casey KS, Schlax MG (2007) Daily high-resolution-blended analyses for sea surface temperature. J Clim 20:5473–5496
Ripley B, Venables B (2023) MASS: support functions and datasets for Venables and Ripley's MASS.R package version 7.3-60. https://CRAN.R-project.org/web/packages/MASS/index.html
Rohatgi A (2025) WebPlotDigitizer, version 5.2. https://automeris.io
Rohner CA, Richardson AJ, Jaine FRA, Bennett MB and others (2018) Satellite tagging highlights the importance of productive Mozambican coastal waters to the ecology and conservation of whale sharks. PeerJ 6:e4161
Røstad A, Kaartvedt S, Aksnes DL (2016) Light comfort zones of mesopelagic acoustic scattering layers in two contrasting optical environments. Deep Sea Res I 113:1–6
Saunders RA, Ratcliffe N, Farrell ED, Clarke MW (2025) Migration and space use by porbeagle sharks *Lamna nasus* in the northeast Atlantic. Mar Ecol Prog Ser 755: 95–114
Sequeira AMM, Mellin C, Meekan MG, Sims DW, Bradshaw CJA (2013) Inferred global connectivity of whale shark *Rhincodon typus* populations. J Fish Biol 82:367–389
Sequeira AMM, Rodríguez JP, Eguíluz VM, Harcourt R and others (2018) Convergence of marine megafauna movement patterns in coastal and open oceans. Proc Natl Acad Sci USA 115:3072–3077
Sigurjónsson J, Víkingsson G (1997) Seasonal abundance of and estimated food consumption by cetaceans in Icelandic and adjacent waters. J Northwest Atl Fish Sci 22: 271–287
Sims DW (1999) Threshold foraging behaviour of basking sharks on zooplankton: life on an energetic knife-edge? Proc R Soc B 266:1437–1443

Sims DW (2008) Sieving a living: a review of the biology, ecology and conservation status of the plankton-feeding basking shark *Cetorhinus maximus*. Adv Mar Biol 54:171–220

Sims DW Merrett DA (1997) Determination of zooplankton characteristics in the presence of surface feeding basking sharks *Cetorhinus maximus*. Mar Ecol Prog Ser 158: 297–302

Sims DW, Quayle VA (1998) Selective foraging behaviour of basking sharks on zooplankton in a small-scale front. Nature 393:460–464

Sims DW, Reid PC (2002) Congruent trends in long-term zooplankton decline in the north-east Atlantic and basking shark (*Cetorhinus maximus*) fishery catches off west Ireland. Fish Oceanogr 11:59–63

Sims DW, Speedie CD, Fox AM (2000) Movements and growth of a female basking shark re-sighted after a three year period. J Mar Biol Assoc UK 80:1141–1142

Sims DW, Southall EJ, Richardson AJ, Reid PC, Metcalfe JD (2003) Seasonal movements and behaviour of basking sharks from archival tagging: no evidence of winter hibernation. Mar Ecol Prog Ser 248:187–196

Sims DW, Southall EJ, Tarling GA, Metcalfe JD (2005) Habitat-specific normal and reverse diel vertical migration in the plankton-feeding basking shark. J Anim Ecol 74:755–761

Sims DW, Witt MJ, Richardson AJ, Southall EJ, Metcalfe JD (2006) Encounter success of free-ranging marine predator movements across a dynamic prey landscape. Proc R Soc B 273:1195–1201

Singh NJ, Börger L, Dettki H, Bunnefeld N, Ericsson G (2012) From migration to nomadism: movement variability in a northern ungulate across its latitudinal range. Ecol Appl 22:2007–2020

Skomal GB, Wood G, Caloyianis N (2004) Archival tagging of a basking shark, *Cetorhinus maximus*, in the western North Atlantic. J Mar Biol Assoc UK 84:795–799

Skomal GB, Zeeman SI, Chisholm JH, Summers EL, Walsh HJ, McMahon KW, Thorrold SR (2009) Transequatorial migrations by basking sharks in the western Atlantic Ocean. Curr Biol 19:1019–1022

Stott FC (1982) A note on catches of basking sharks, *Cetorhinus maximus* (Gunnerus), off Norway and their relation to possible migration paths. J Fish Biol 21:227–230

Thieurmel B, Elmarhraoui A (2022) suncalc: compute sun position, sunlight phases, moon position and lunar phase. R package version 0.5.1. https://CRAN.R-project.org/web/packages/suncalc/index.html

Thorburn J, Collins PC, Garbett A, Vance H and others (2024) Assessing the potential of acoustic telemetry to underpin the regional management of basking sharks (*Cetorhinus maximus*). Anim Biotelem 12:20

Vandeperre F, Aires-da-Silva A, Fontes J, Santos M, Santos RS, Afonso P (2014) Movements of blue sharks (*Prionace glauca*) across their life history. PLOS ONE 9:e103538

Vaudo JJ, Byrne ME, Wetherbee BM, Harvey GM, Shivji MS (2017) Long-term satellite tracking reveals region-specific movements of a large pelagic predator, the shortfin mako shark, in the western North Atlantic Ocean. J Appl Ecol 54:1765–1775

Waller MJ, Humphries NE, Womersley FC, Loveridge A and others (2024) The vulnerability of sharks, skates, and rays to ocean deoxygenation: physiological mechanisms, behavioral responses, and ecological impacts. J Fish Biol 105:482–511

Weng KC, Foley DG, Ganong JE, Perle C, Shillinger GL, Block BA (2008) Migration of an upper trophic level predator, the salmon shark *Lamna ditropis*, between distant ecoregions. Mar Ecol Prog Ser 372:253–264

Wikelski M, Tarlow EM, Raim A, Diehl RH, Larkin RP, Visser GH (2003) Costs of migration in free-flying songbirds. Nature 423:704

Appendix. Full list of author addresses

C. Antonia Klöcker[1,2], Martin C. Arostegui[3], Keno Ferter[1], Otte Bjelland[1], Mauvis A. Gore[4,5], Jan Hinriksson[1], Robert J. Lennox[6], Petter Lundberg[7], Peter I. Miller[8], Axel Schlindwein[9], Lara L. Sousa[10,11,12], David W. Sims[13,14], Nuno Queiroz[10,11], Claudia Junge[1]

[1]Havforskningsinstituttet (Institute of Marine Research, IMR), 5005 Bergen, Norway

[2]Department of Biosciences, University of Oslo, 0316 Oslo, Norway

[3]Biology Department, Woods Hole Oceanographic Institution, Woods Hole, MA 02543-1050, USA

[4]Marine Conservation International, Isle of Mull PA72 6JP, UK

[5]Institute of Life and Earth Sciences, School of Energy, Geoscience, Infrastructure and Society, Heriot-Watt University, Edinburgh EH14 4AS, UK

[6]Ocean Tracking Network, Dalhousie University, Halifax, NS B3H 4R2, Canada

[7]Department of Wildlife, Fish, and Environmental Studies, Swedish University of Agricultural Sciences, Umeå 901 83, Sweden

[8]Plymouth Marine Laboratory, Prospect Place, Plymouth PL1 3DH, UK

[9]UiT The Arctic University of Norway, 9037 Tromsø, Norway

[10]CIBIO, Centro de Investigação em Biodiversidade e Recursos Genéticos, InBIO Laboratório Associado, Campus de Vairão, Universidade do Porto, 4485-661 Vairão, Portugal

[11]BIOPOLIS Program in Genomics, Biodiversity and Land Planning, CIBIO, Campus de Vairão, 4485-661 Vairão, Portugal

[12]Wildlife Conservation Research Unit, Department of Biology, University of Oxford, Oxford OX1 3EL, UK

[13]Marine Biological Association, The Laboratory, Citadel Hill, Plymouth PL12PB, UK

[14]Ocean and Earth Science, National Oceanography Centre Southampton, University of Southampton, Southampton SO14 3ZH, UK

Editorial responsibility: Myron Peck, Den Burg, The Netherlands
Reviewed by: 3 anonymous referees
Submitted: June 16, 2025; Accepted: March 10, 2026
Proofs received from author(s): May 8, 2026